Crystallization Kinetics of Glass Fiber Reinforced PBT Composites

CHAN-SEOK PARK,[1] KI-JUN LEE,[1] JAE-DO NAM,[2] SEONG-WOO KIM[3]

[1] Division of Chemical Engineering, Seoul National University, Seoul 151-742, Korea

[2] Department of Polymer Science and Engineering, Sung Kyun Kwan University, Suwon, 440-746, Korea

[3] Department of Chemical Engineering, Kyonggi University, Suwon, 442-760, Korea

Received 9 September 1999; accepted 2 February 2000

ABSTRACT: The effect of glass fibers on the crystallization of poly(butylene terephthalate) (PBT) was investigated by crystallization kinetics analysis under isothermal and nonisothermal conditions. From the crosspolar optical micrographs of melt- and solvent-crystallized PBT composites, the glass fibers were found to increase the number density and decrease the size of crystallites. The glass fibers provided heterogeneous nucleation sites, and thus enhanced the overall rate of PBT crystallization in isothermal experiments. However, the Avrami exponent and the regime transitions were not significantly affected by the presence of glass fibers. For the nonisothermal kinetics of PBT composites, the model prediction was excellent in most ranges of crystallization, but it deviated above 70% of crystallization especially at fast cooling rates (>40°C/min). This discrepancy of the model seemed to result from the growth regime transitions, which were clearly observed especially at high undercoolings. © 2000 John Wiley & Sons, Inc. J Appl Polym Sci 78: 576–585, 2000

Key words: crystallization kinetics; crystalline growth; regime transitions; glass fiber reinforced poly(butylene terephthalate)

INTRODUCTION

In crystalline thermoplastics, the crystalline morphology and the degree of crystallinity are the most important variables in determining mechanical and physical properties of the final products. The crystallization of these polymers is often influenced not only by processing conditions, but also by the presence of the reinforcing phases. Accordingly, a comprehensive understanding of the interactions between the fiber and matrix is required for the development of crystalline thermoplastic composite systems.[1]

The fiber surfaces involved in crystallizable polymers generally favor heterogeneous nucleation by acting as nucleating sites for crystallization. The existence of transcrystalline zone occurring along the fiber surface with a sufficiently high density has been reported to depend on the types of fibers and polymers.[1–7] In the case of glass fiber-reinforced thermoplastic composites, however, the transcrystalline zone was not always observed around the fiber surfaces,[8–10] although the nucleation density is increased due to the glass fibers.

PBT is one of the fastest crystallizing polymers among the polyesters, and does not usually require nucleation agents.[11,12] It is particularly well suited for injection-molding applications because the high rates of crystallization ensure short processing cycles and excellent thermodynamically

Correspondence to: K.-J. Lee.

Journal of Applied Polymer Science, Vol. 78, 576–585 (2000)

and dimensionally stable parts. The glass fiber-reinforced PBT grades generally provide good mechanical stiffness and strength at elevated temperatures. Even for the wide range of applications, however, the crystallization kinetics of PBT and glass fiber-reinforced PBT composites have not been investigated as extensively.[13]

The purpose of this article is to examine the crystallization kinetics of PBT composites using differential scanning calorimetry (DSC) under isothermal and nonisothermal conditions. The kinetic model parameters were used to quantitatively identify the effects of glass fibers on the crystallization behaviors of PBT composites. The crystalline morphologies of the glass fiber PBT composites were also investigated by using a crosspolar optical microscopy technique.

Crystallization Kinetics

The crystallization kinetics of crystalline thermoplastic materials is often studied under isothermal conditions by using DSC. The general Avrami equation may be utilized to describe the crystallization rate of thermoplastic polymers:[14]

$$\frac{X(t)}{X_\infty} = 1 - \exp(-kt^n) \tag{1}$$

where $X(t)$ is the absolute crystallinity at time t, X_∞ is the ultimate absolute crystallinity, k is a rate constant involving both nucleation and growth rate parameters under isothermal condition, and n is the exponent, which may be referred to the specific mechanism of nucleation and the geometry and the kinetics of crystal growth.

The temperature dependence of crystal growth rates may also be described by the theory of Lauritzen and Hoffman.[15] For the analysis of DSC experimental results, the linear growth rate may be expressed by the apparent rate of crystallization to reach a specific level of crystallization, for example, 50% of crystallization, viz:

$$\left(\frac{1}{t_{1/2}}\right) = \left(\frac{1}{t_{1/2}}\right)_0 \exp\left(\frac{U^*}{R_g(T - T_\infty)}\right)\exp\left(-\frac{K_g}{T\Delta Tf}\right) \tag{2}$$

where $t_{1/2}$ is the time required to attain 50% conversion, $(1/t_{1/2})_0$ is a constant, U^* is a constant for short-distance diffusion of the crystallizing segments, R_g is the gas constant, T is the crystallization temperature, T_∞ is a temperature that is related to the glass transition temperature, K_g is the nucleation kinetic constant that depends on the surface energy of crystals and the mechanisms of crystallization, ΔT is the degree of undercooling ($=T_m^o - T$, where T_m^o is the equilibrium melting point), and f is a correction factor close to unity that takes into account of changes in the heat of fusion with temperature.

Crystallization of polymers and composites inevitably occurs during polymer processing under nonisothermal conditions. There have been various modifications of Avrami crystallization kinetic model for nonisothermal crystallization conditions. Based on the assumptions that the number of activated nuclei is constant in isokinetic conditions, Nakamura et al.[16] extended the Avrami theory for nonisothermal crystallization as follows:

$$\frac{d\theta}{dt} = nK(T)(1 - \theta)[-\ln(1 - \theta)]^{n-1/n} \tag{3}$$

where $\theta = X(T)/X_\infty$, indicating a relative crystallinity, and $K(T)$ is the nonisothermal crystallization rate constant related to the Avrami isothermal crystallization rate constant, $k(T)$, by $K(t) = [k(T)]^{1/n} = (\ln 2)^{1/n}\,(1/t_{1/2})$.

As proposed by Sifleet et al.[17] and other researchers,[18–20] the crystallization induction time may be defined by the time when the crystallization actually starts. According to this approach, the nonisothermal induction time is obtained by an integration of isothermal induction times as following, which often evaluated by a summation of discrete isothermal induction times:

$$\int_0^{t_I} \frac{dt}{t_i(T)} = 1 \tag{4}$$

where t_i is the isothermal induction time, and t_I is the nonisothermal induction time. For melt crystallization, the isothermal induction time may be assumed to comply with the expression proposed by Godovsky and Slonimsky:[21]

$$t_i = t_m(T_m^0 - T)^{-a} \tag{5}$$

where t_m and a are material constants, which are independent of temperature.[19,20] Using eq. (5), the nonisothermal induction time may be obtained by an analytic integration of eq. (4).

EXPERIMENTAL

Materials

The glass fiber contents used in this study were 0, 10, 20, and 30 wt %, each referred to as PBT0, PBT10, PBT20, and PBT30, respectively [LG Chem. Co.]. The fiber length was measured by using an image analyzer of optical microscope photographs, which were taken after the polymer was removed by a 10% solution of TFA in CCl_4. The fiber diameter was about 10 μm and the average length was 0.309 mm. PBT composite specimens were dried in a vacuum oven at 80°C for 24 h before experiments.

Microscopy

For polarized light microscopy investigation, thin films of about 20 to 50 μm in thickness were prepared by pressing a pellet of PBT between two thin cover glasses in a Carver press. The specimen was aged at 270°C for 10 min and quenched in ice-water or cooled in air. The PBT films were also prepared by a solvent-casting method from a 10% solution of TFA in CCl_4. The crystalline structures of the specimens were examined by a polarizing light microscope.

Thermal Analysis

For isothermal crystallization analysis, the samples were first heated to 270°C and kept for 10 min in the Perkin-Elmer 7 differential scanning calorimeter (DSC) cell. Then, the melted specimens were cooled down at 80°C/min to the desired crystallization temperature (T_c) and kept isothermally for a desired period of time. The isothermal crystallization kinetic experiments were carried out in temperatures between 180 and 210°C in this study.

For nonisothermal experiments, the specimen was heated from 30 to 270°C at 20°C/min and held at that temperature for 10 min. Then they were cooled at different cooling rates of 1, 5, 10, 20, 40, and 80°C/min to room temperature. For the measurement of thermal effects in polymers, as associated with melting, crystallization, and glass transition, the effect of temperature lag in DSC may be considered. In this study, however, the effect was not included, because we were interested in relative comparison of the crystallization rates of PBT composite systems. Further research is needed on this subject.

RESULTS AND DISCUSSION

Morphology

Figure 1 shows the crosspolar optical micrographs of melt-crystallized PBT composites. Figure 1(a) and (b) presents the pictures of the ice-water–quenched films, and (c) and (d) the air-cooled films. As expected, we can see that the glass fibers provide nucleating sites when they are used as a PBT composite reinforcement. It is seen that PBT0 contains relatively large crystals, whereas a dense granular texture of crystals is formed in the presence of glass fibers. The number density around the fiber surface is much greater than in the bulk, but the size of spherulites on the fiber surfaces is very smaller. However, although the nucleating effect of glass fibers is observed, the transcrystalline zone is not clearly observed in melt-crystallized PBT films. This may indicate that the nucleation density is increased by the fiber surface, but not sufficiently enough to form transcrystalline layers. This result is agreed well with other investigations.[8–10]

It should also be mentioned that the spherulite size of films quenched in ice water [Fig. 1(a) and (b)] is much smaller than that quenched in air [Fig. 1(c)and (d)]. This seems to result from the effective cessation of spherulite growth by the rapid cooling in ice water. It demonstrates that the crystalline morphology of PBT systems is strongly affected by processing cooling conditions.

From the examination of solvent-crystallized samples, we may also confirm that the glass fibers provide nucleation sites for the PBT matrix (Fig. 2). It should also be noted that the spherulitic morphologies obtained from the solvent and melt-crystallized films may be quite different. In this observation, thin films of semicrystalline polymers in polarizing light show dark maltese crosses in the spherulitic structure. In melt-crystallized PBT films [Fig. 1(a) to (d)], the maltese crosses exhibit about 45° to the polarizers, known as the unusual type. This unusual type is a characteristic of spherulites whose optical axis lies at an angle of approximately 45° to the spherulitic radius.[13,22–23] On the other hand, as seen in the solvent-crystallized PBT films (Fig. 2), the maltese crosses are along the polar directions (0–90°) under the polarized microscope, referred to as the usual type. This arises from spherulites containing their optical axis either along or perpendicular to the spherulitic radius. These results indicate that the bulk structure or macrostructure of

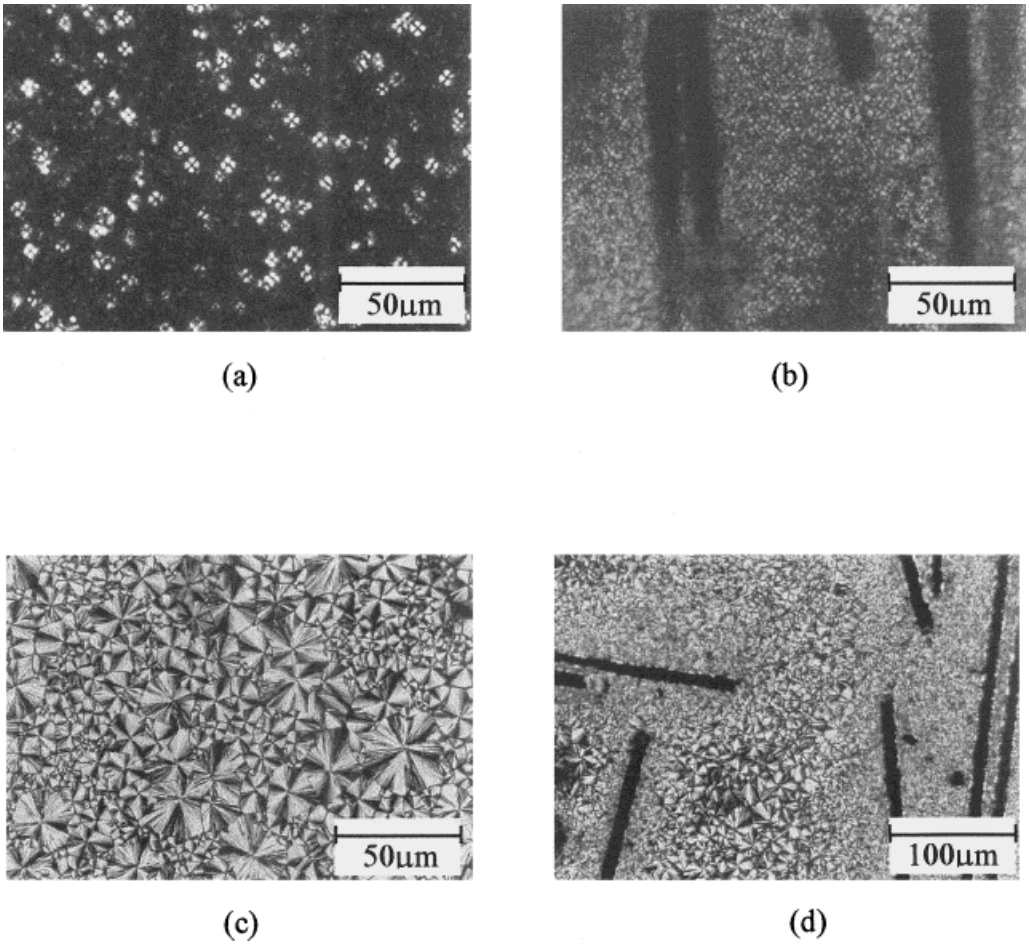

Figure 1 Optical micrographs of melt-crystallized films of PBT0 in (a) and (c), and PBT30 in (b) and (d).

the PBT systems depends on whether the crystallization occurs from dilute solutions or from melts.

Isothermal Crystallization

The total heat evolved during crystallization was measured by using DSC. This includes the heat resulting from both nucleation and growth processes. Typical experimental crystallization isotherms are shown in Figure 3 for PBT composite systems at the crystallization temperature of 200°C. As expected, the increased amount of glass fibers decreases the crystallization time; i.e., the crystallization rate of PBT composites is increased with glass fibers, seemingly because the glass fibers provide nucleating sites. This supports the morphological observations for the glass fiber filled PBT systems in Figures 1 and 2.

The isothermal induction times, t_i, for PBT composite systems are shown in Figure 4. As can be seen, the influence of the glass fibers on t_i is clearly demonstrated, and is especially pronounced at higher T_c. This may be the reason that the glass fibers enhance the nucleation ability and the possibility of heterogeneous nucleation of PBT polymers. In addition, the isothermal induction time parameters were obtained by fitting eq. (5) to the experimental data. These results are listed in Table I.

The overall rate of crystallization may be expressed in terms of the crystallization half-time, $t_{1/2}$, when 50% of the total crystallization is reached. Figure 5 gives $t_{1/2}$ of PBT composites as a function of isothermal crystallization temperature. As can be seen, the crystallization temperature leads to an increase in $t_{1/2}$ in an accelerating way. Therefore, the rate of crystallization, which

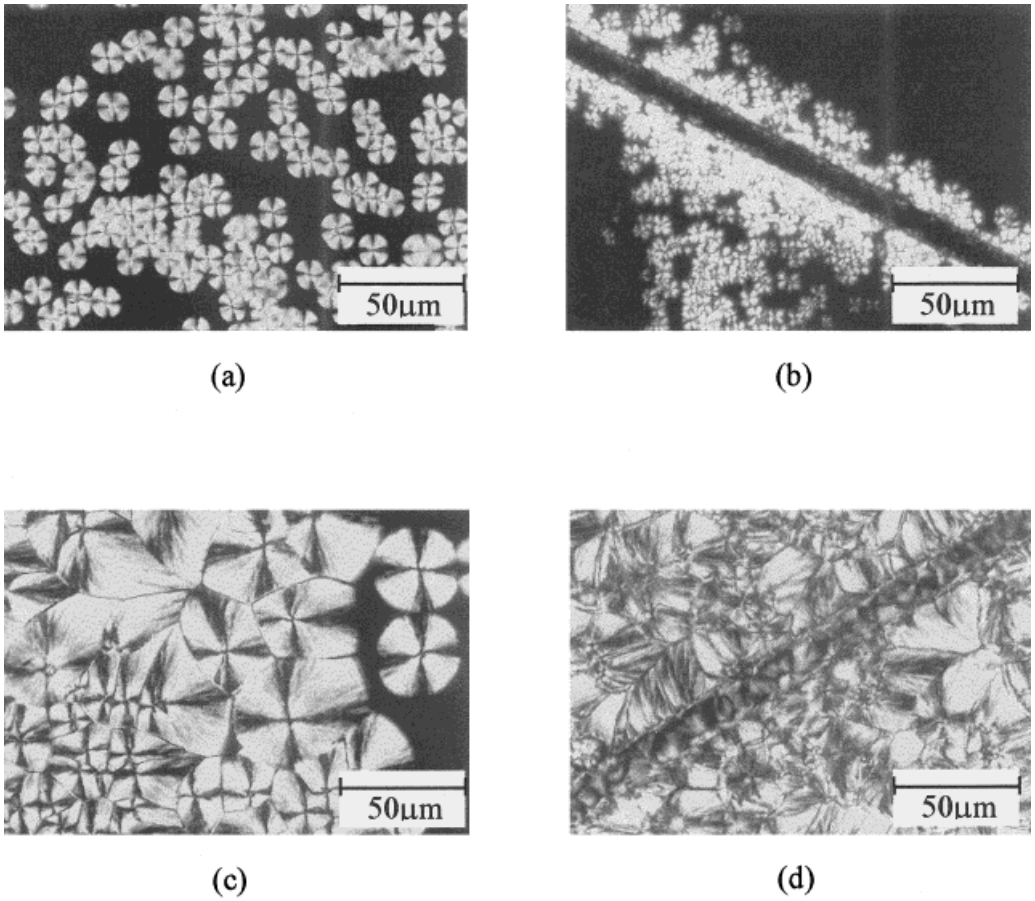

Figure 2 Optical micrographs of solvent-crystallized films of PBT0 in (a) and (c), and PBT30 in (b) and (d).

may be represented by the inverse of $t_{1/2}$, is increased with the increase of the degree of undercooling, ΔT. Figure 5 also shows that the crystallization rate increases with the addition of glass fibers, which directly increases the number of heterogeneous nucleation sites while the crystalline growth rate may be independent of glass fibers.

The model parameters of the Avrami eq. (1) can be obtained from the plots of $\log[-\ln(1-\theta)]$ vs. $\log(t)$. In our results, the slope n was found to vary

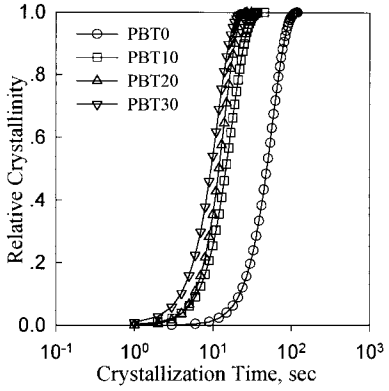

Figure 3 Isothermal crystallization of PBT composite systems at 200°C.

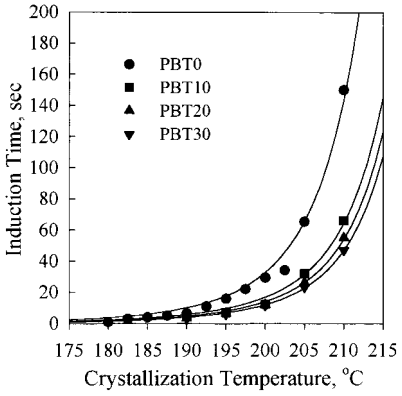

Figure 4 Isothermal induction times of PBT composite systems. Lines represent the nonlinear regressions.

Table I The Kinetic Parameters for Isothermal Crystallization of PBT Composite Systems

	t_m ($\times 10^{10}$) (sK^a)	a	n	$\ln(1/t_{1/2})_{OI}$ (s^{-1})	$\ln(1/t_{1/2})_{OII}$ (s^{-1})	K_{gI} ($\times 10^5$) (K^2)	K_{gII} ($\times 10^5$) (K^2)
PBT0	16.05	5.86	2.30	17.83	8.32	3.60	1.58
PBT10	1.01	5.31	2.49	14.31	7.37	2.63	1.22
PBT20	1.01	5.36	2.51	14.05	7.29	2.60	1.17
PBT30	1.00	5.39	2.49	13.96	7.24	2.55	1.12

somewhat with temperature, and the average value of n for PBT composite systems are summarized in Table I. As can be seen, no evident trend of the values of n with the quantity of glass fibers is noticed. Therefore, it may be reasonable to consider that the glass fibers do not affect the geometric dimension of PBT crystal growth. While n may be considered as a constant with temperatures, k depends strongly on T_c. The isothermal rate constants, k, are also shown in the Figure 5 as a function of T_c for various quantity of glass fibers. It can be seen that the values of k, indicating the crystallization rates, increase with the degree of undercooling, and also with the glass fiber contents. It agrees well with the previous results of the crystallization half-time.

In this study, the Hoffman-Lauritzen analysis was used to determine the temperature variation of the overall rate of crystallization ($1/t_{1/2}$). The kinetic parameters of eq. (2) may be obtained by plotting $\ln(1/t_{1/2}) + U^*/R(T-T_\infty)$ vs. $1/(T(Tf)$. According to Hoffman et al., the U^* and T_∞ may be assigned as "universal" values of 6400J/mol and $T_g - 30$ K, respectively, T_g being the glass transition temperature.[15] In this study, the glass transition temperature and the equilibrium melting point of PBT composite systems were taken as 28°C[13] and 24°C,[24] respectively. Figure 6 represents the results of the Hoffman-Lauritzen plot of our PBT composites exhibiting two distinct crystallization stages with a transition at T_c = 195°C. According to the Hoffman-Lauritzen kinetic theory, this transition may be attributed to a change in the growth regime.[25] The regime transition occurs due to the relative-rate changes between the growth rate and the surface nucleation rate of a crystallite, which are generally associated with the degree of undercoolings.[26] Three regimes of crystallization kinetics have been proposed on both theoretical and experimental grounds as discussed in detail in the literature.[22,25] The presence of a transition from regime I to regime II crystallization has been reported as a sharp and distinct change from axialitic to spherulitic supermolecular structures.[22,26–28] A list of references regarding the regime transitions has been provided by Hoffman and Miller.[29]

In this study, the transition in Figure 6 may be referred to a transition from regime I at higher temperatures to regime II at lower temperatures. The crystallization rate could be obtained over a

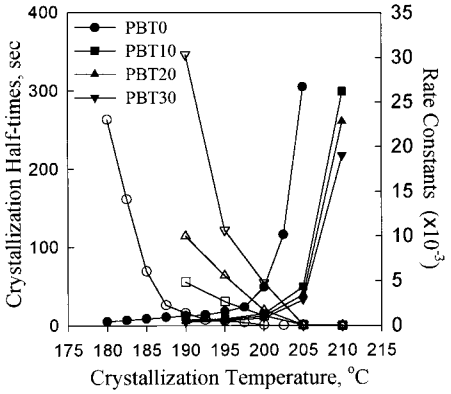

Figure 5 Crystallization half-times($t_{1/2}$) and isothermal rate constants(k) of PBT composite systems as a function of crystallization temperature. Represented by filled symbols for $t_{1/2}$ and open symbols for k.

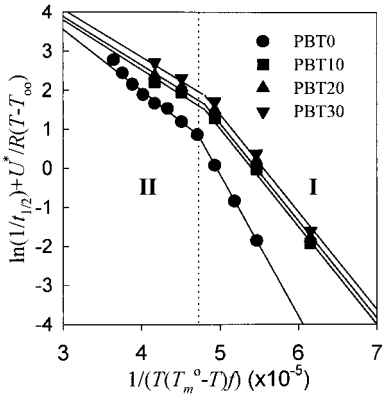

Figure 6 Hoffman-Lauritzen plots for PBT composite systems.

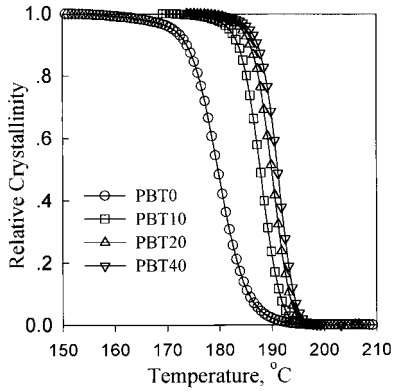

Figure 7 Relative crystallinity of PBT composite systems as a function of temperature measured at 40°C/min of cooling rate.

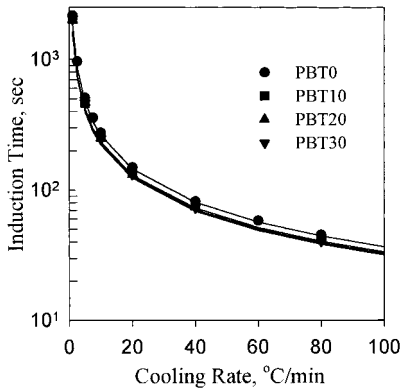

Figure 8 Nonisothermal induction times of PBT composite systems. Lines represent the model fittings.

narrow range of temperatures in this study (i.e., at a relatively low degree of undercooling) due to the fast crystallization characteristics of PBT. This may be the reason why we could not observe the transition from Regime II to Regime III.

The parameter values of $(1/t_{1/2})_0$ and K_g at each regime are summarized in Table I. It should be mentioned that the ratios of the nucleation constants, K_{gI}/K_{gII}, are approximately 2.2 for all PBT composites, which is close to the theoretical estimate.[25] Table I presents the effect of glass fiber on the crystalline nucleation of PBT. The addition of glass fiber into PBT decreases the values of K_{gI} and K_{gII}, which seems to indicate that glass fibers lower the energy required to form a crystal nucleus of critical size. The reduction in the values $(1/t_{1/2})_0$ associated with the addition of glass fibers may be attributed to a reduction of interfacial surface energies.

Nonisothermal Crystallization

The relative crystallinity of PBT composites measured in nonisothermal conditions are shown in Figure 7 at a cooling rate of 40°C/min. As can be seen, the onset temperature shifts to higher temperatures with the increased glass fiber contents, and the degree of crystallinity of glass fiber-reinforced PBT is higher than that of neat PBT at the same temperature. This may indicate that the presence of glass fibers initiate the nucleation of PBT under the nonisothermal conditions, and that the increased nucleation sites lead to an increase in the overall rate of crystallization.

The nonisothermal induction times, t_I, for PBT composite systems are shown Figure 8. The model parameters were obtained by a nonlinear regression method using the isothermal data, and were subsequently used for the fit of the nonisothermal induction times. It can be seen that eq. (4) compares well with the nonisothermal induction times for all PBT composite systems.

In Figure 9, the dynamic crystallization rates, defined as a inverse of the crystallization half-time, $t_{1/2}$, are compared as a function of cooling rates for various glass fiber contents of PBT composites. The crystallization rate is strongly dependent on cooling rates, and evidently exhibits a higher value for higher glass fiber contents. In addition, this behavior is predominant in the case of fast cooling rates. At slow cooling rates, the effect of glass fiber contents on the crystallization rates does not appear significant for all PBT composite systems. At a rapid cooling rate, however, the increased rate of crystallization results from an increased nucleation density, and thus a little time is allowed for the development of crystalline entities at rapid cooling rates. This can also be

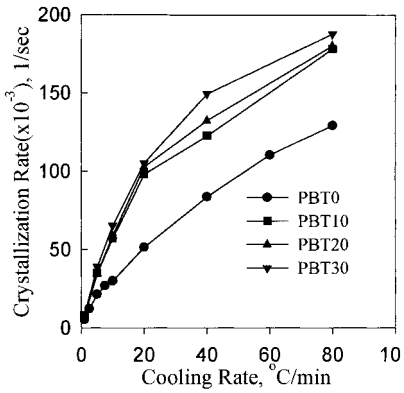

Figure 9 Nonisothermal crystallization rates of PBT composites as a function of cooling rate.

Table II Values of K_0 ($\times 10^6$) for PBT Composites Obtained by Using the Isothermal Nucleation Constants in the Regime I, K_{gI}, as Listed in Table I

Cooling Rate (°C/min)	PBT0	PBT10	PBT20	PBT30
1	1940	78.5	80.0	49.1
5	1590	56.1	53.4	49.9
10	783	42.7	51.0	44.5
20	292	29.5	39.1	34.4
40	175	16.8	21.8	22.4
80	157	9.1	9.2	10.3

confirmed by the microscopic observation of the melt-crystallized PBT morphologies in Figures 1 and 2. At slow cooling rates, crystallites may have enough time to develop into the principal lamellae of spherulites, and thus the size of crystallites become larger. Consequently, it may be reasonable to consider that the nucleating capability of glass fiber is increased with the cooling rates.

Nonisothermal crystallization kinetics of thermoplastic systems is of importance in process modeling and crystallization control.[19,30] Patel and Spruiell used a nonlinear regression method to directly fit the nonisothermal data to Nakamura model. Recently, the kinetic parameters derived from isothermal experiments were also used to predict the nonisothermal crystallization behavior. In the present study, however, we realized that the Avrami exponent could be assumed to be independent of temperature, but the other parameters of $(1/t_{1/2})_0$ and K_g were determined as different values in two growth regimes. In addition, it should be mentioned that the regime III was not considered in this study, but it may exist in lower temperature regions of crystallization, as theoretically predicted by Hoffman-Lauritzen. These regime transitions of crystallization processes may cause significant discrepancies of mathematical modeling in nonisothermal kinetic analysis.

To obtain kinetic parameters applicable for various thermal conditions, Nakamura's eq. (3) was incorporated with Hoffman-Lauritzen's eq. (2) in this study. The differential form of the Nakamura model may be simplified by letting $Y = \ln[1/(1-\theta)]$, which desirably eliminates the possibility for θ to be greater than 1 in solving the differential equation.[30] Consequently, the nonlinear differential equation becomes:

$$\frac{dY}{dt} = nK(T)Y^{(n-1)/n} \tag{6}$$

where

$$K(T) = K_0 \exp\left(-\frac{U^*}{R_g(T - T_\infty)}\right)\exp\left(-\frac{K_g}{T\Delta Tf}\right) \tag{7}$$

and where $K_0 = (\ln 2)^{1/n}(1/t_{1/2})_0$.

Using K_{gI} and K_{gII}, which were already determined in isothermal experiments, K_0 was obtained by a nonlinear regression method, and summarized in Tables II and III for different regimes with various cooling rates. When K_{gI} is used for the model description, K_0 decreases with cooling rates as shown in Table II. On the other hand, when K_{gII} is used, K_0 increases with cooling rates for all PBT composite systems, as shown in Table III. In this study, we took the values of K_{gI} and K_{gII} as upper and lower limits, and numerically estimated a representative value K_g by using a successive iteration method to minimize the standard deviation of K_0. Consequently, the model parameters of K_g and K_0 are listed in Table IV. Figure 10 collectively compares the model predictions of eqs. (6) and (7) with nonisothermal experimental data for PBT20 system. They compare very well but deviate in the range of $\theta > 0.7$, especially at cooling rates higher than 40°C/min. A similar trend was also observed for PBT0, PBT10, and PBT30, which was not included here.

In previous studies, it has been reported that the nucleation constants for regimes I and III are the same, but they are twice higher than that for regime II, i.e., $K_{gI} = 2K_{gII} = K_{gIII}$.[25] Therefore, it may be reasonable for a representative value of K_g to be between the values of K_{gI} and K_{gII} for describing the nonisothermal kinetics. However,

Table III Values of K_0 ($\times 10^6$) for PBT Composites Obtained by Using the Isothermal Nucleation Constants in the Regime II, K_{gII}, as Listed in Table I

Cooling Rate (°C/min)	PBT0	PBT10	PBT20	PBT30
1	0.034	0.016	0.018	0.009
5	0.075	0.031	0.034	0.023
10	0.084	0.032	0.049	0.031
20	0.071	0.058	0.056	0.039
40	0.082	0.048	0.059	0.045
80	0.120	0.048	0.049	0.040

Table IV Optimum Kinetic Parameters for Prediction of Nonisothermal Crystallization of PBT Composite Systems

	K_0 ($\times 10^6$) (s^{-1})	K_g ($\times 10^5$) (K^2)
PBT0	2.71	2.40
PBT10	2.64	2.11
PBT20	2.17	2.02
PBT30	1.68	1.95

the preexponential factor, $(1/t_{1/2})_0$, for regime III has been reported to be substantially small compared to regime I.[25] Accordingly, the model parameter K_0, which is closely associated with $(1/t_{1/2})_0$ seemed to cause the deviation specifically in the region $R > 40$°C/min and $\theta > 0.7$ in our model predictions.

The master curves for nonisothermal crystallization data was constructed by using a method developed by Chan et al.[31] The shift factors of our PBT composites are shown in Figure 11, and the master curves in Figure 12 for nonisothermal crystallization. Figure 11 represents shift factors of PBT composite systems obtained from the dynamic crystallization data, with a reference temperature of 200°C and a reference cooling rate of 10°C/min. The shift factors compare well with the Hoffman-Lauritzen expression, of which model parameters were already determined in Table IV. It is interesting to note that the superposition seems quite good, but the Hoffman-Lauritzen equation seems to deviate at temperatures lower than 195°C, which may be attributed to a transition temperature between regime I and II. Overall, the model prediction and the master curves of the nonisothermal crystallization behavior may well be described by our crystallization analysis methodology in a broad range of cooling rates and various composite systems.

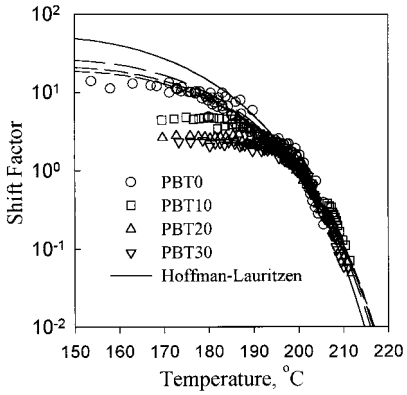

Figure 11 Shift factors as a function of temperature for PBT composite systems.

CONCLUSIONS

The crosspolar optical micrography was used to investigate the crystalline morphology of PBT composite systems crystallized from melts. The glass fibers increased the number density and decreased the size of crystallites, indicating that the glass fibers act as nucleation sites. However, the transcrystalline layer was not clearly observed at the vicinity of the glass fiber surfaces.

Analyzing the crystallization half-time of isothermal and nonisothermal conditions, the overall rate of crystallization was increased for the

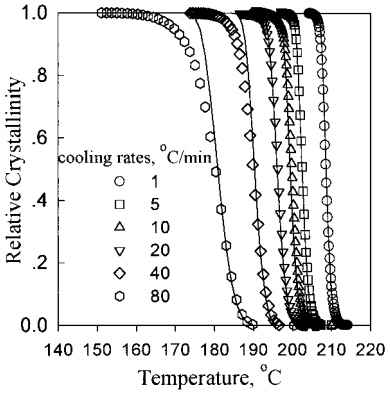

Figure 10 Relative crystallinity of PBT20 as a function of temperature. Lines represent the model predictions.

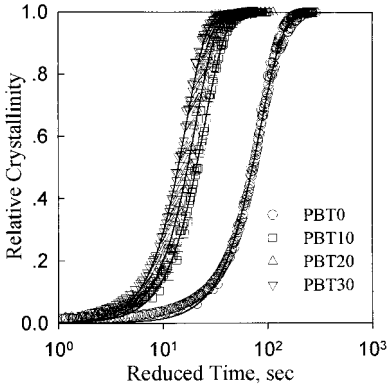

Figure 12 Master curves as a function of reduced time for PBT composites under nonisothermal crystallization.

increased glass fiber contents, which seemed to result from the increased nucleation density due to the presence of glass fiber. This was also supported by the analyses of Avrami and Hoffman-Lauritzen models. In particular, the addition of glass fibers into the PBT matrix decreased the values of the nucleation constants, $K_{g\mathrm{I}}$ and $K_{g\mathrm{II}}$, which means that glass fibers lower the energy required to form a crystal nucleus of critical size. While the nucleation was affected by the presence of glass fiber, the growth mechanism of crystallites was seemingly not affected. This was supported by the fact that the Avrami exponent, n, was nearly constant for various amounts of glass fibers and the crystallization transition was observed for all PBT composite systems at a constant temperature of 195°C. The model prediction compared the nonisothermal experimental data very well for a broad range of cooling rates, except when the crystallinity was specifically above 0.7 at higher cooling rates ($R > 40$°C/min), seemingly corresponding to another transition from regime II to regime III.

REFERENCES

1. Burton, R. H.; Folkes, M. J. Mechanical Properties of Reinforced Thermoplastics; Clegg, D. W.; Collyer, A. A., Ed.; Elsevier Appl. Sci.: London, 1986.
2. Cambell, D.; Qayyum, M. M. J Polym Sci Polym Phys Ed 1984, 18, 83.
3. Ishida, H.; Bussi, P. Macromolecules 1991, 24, 3569.
4. Lustiger, A. Polym Compos 1992, 13, 408.
5. Thomason, J. L.; Von Rooyen, A. A. J Mater Sci 1992, 27, 889.
6. Varga, J.; Karger-Kocsis, J. Polym Bull 1993, 30, 105.
7. Wu, C. M.; Chen, M.; Karger-Kocsis, J. Polym Bull 1998, 41, 239.
8. Avela, M.; Martuscelli, E.; Sellitt, C.; Garagnani, E. J Mater Sci 1987, 22, 3185.
9. Devaux, J.; Chabert, B. Polym Commun 1990, 31, 391.
10. Janevski, A.; Bogoeva-Gaceva, G. J Appl Polym Sci 1998, 69, 381.
11. Werner, E.; Janocha, S.; Hopper, M. J.; Mackenzie, K. J. Encyclopedia of Polymer Science and Engineering; Kroschwitz, J. I., Ed.; Wiley-Interscience: New York, 1988, vol.. 12.
12. Gilbert, M.; Hybart, F. J. Polymer 1972, 13, 327.
13. Stein, R. S.; Misra, A. J Polym Sci Polym Phys Ed 1980, 18, 327.
14. Avrami, M. J Chem Phys 1941, 9, 1977.
15. Hoffman, J. K.; Davis, G. T.; Lauritzen, J. I. Treatise on Solid State Chemistry: Crystalline and Noncrystalline Solids; Hannay, N. B., Ed.; Plenum: New York, 1976, vol. 3.
16. Nakamura, K.; Katayama, K.; Amano, T. J Appl Polym Sci 1973, 17, 1031.
17. Sifleet, W. L.; Dinos, N.; Collier, J. R. Polym Eng Sci 1973, 13, 10.
18. Hsiung, C. M.; Cakmak, M. Polym Eng Sci 1991, 31, 1372.
19. Chan, T. M.; Isayev, A. I. Polym Eng Sci 1994, 34, 461.
20. Iasyev, A. I.; Chan, T. W.; Shimojo, K.; Gmerek, M. J Appl Polym Sci 1995, 55, 807.
21. Godovsky, Y. K.; Slonimsky, G. L. J Polym Sci Polym Phys Ed 1974, 12, 1053.
22. Gedde, U. W. Polymer Physics; Chapman & Hall: London, 1995.
23. Stein, R. S. Structure and Properties of Polymer Films; Lenz, R. W.; Stein, R. S., Ed.; Plenum: New York, 1973.
24. Cheng, S. Z. D.; Pan, R.; Wunderlich, B. Makromol Chem 1988, 189, 2443.
25. Clark, E. J.; Hoffman, J. D. Macromolecules 1984, 17, 878.
26. Hoffman, J. D.; Frolen, L. J.; Ross, G. S.; Lauritzen, J. I., Jr. J Res Natl Bur Std Phys Chem 1975, 79A, 671.
27. Vasanthakumari, R.; Pennings, A. J. Polymer 1983, 24, 175.
28. Monasse, B.; Ferrandez, P.; Delamare, F.; Montmitonnet, P.; Haudin, J. M. Polym Eng Sci 1987, 37, 1684.
29. Hoffman, J. D.; Miller, R. L. Macromolecules 1989, 22, 3502.
30. Patel, P. M.; Spruiell, J. E. Polym Eng Sci 1991, 31, 730.
31. Chan, T. V.; Shyu, G. K.; Isayev, A. I. Polym Eng Sci 1995, 35, 733.